Chinese J. Chem. Eng., **14**(5) 634—641 (2006)

Turbulence Characteristics of Swirling Reacting Flow in a Combustor with Staged Air Injection*

ZHANG Jian(张健)**, **PU Yong**(普勇) **and ZHOU Lixing**(周力行)
Department of Engineering Mechanics, Tsinghua University, Beijing 100084, China

Abstract This paper presents an experimental investigation of the turbulent reacting flow in a swirl combustor with staged air injection. The air injected into the combustor is composed of the primary swirling jet and the secondary non-swirling jet. A three dimension-laser particle dynamic analyzer (PDA) was employed to measure the instantaneous gas velocity. The probability density functions (PDF) for the instantaneous gas axial and tangential velocities at each measuring location, as well as the radial profiles of the root mean square of fluctuating gas axial and tangential velocities and the second-order moment for the fluctuating gas axial and tangential velocities are obtained. The measured results delineate the turbulence properties of the swirling reacting flow under the conditions of staged combustion.
Keywords swirling reacting flow, staged combustion, turbulence characteristics

1 INTRODUCTION

Swirl combustion is found in a wide variety of thermal power engineering devices including swirl combustors, cyclone combustors, and swirl burners. Swirl provides an effective aerodynamic means to stabilize the flame, control the combustion process, enhance the heat and mass transfer, prolong the fuel residence time, and increase the combustion efficiency[1,2]. For achieving good combustion performance as well as low pollutant emission, swirl should be properly utilized and controlled. Swirl combustion has to be integrated with other combustion techniques. Among them, staged combustion is adopted in many swirl combustor and burners[3,4]. It could be realized by utilizing staged air injection.

Many experimental studies on turbulent reacting flows in swirl combustors have been conducted by employing a laser Doppler anemometer (LDA) system[5—12]. Detailed distributions of the time-averaged and fluctuating gas axial, radial, and tangential velocities and the probability density functions (PDF) for instantaneous gas axial and tangential velocities are obtained under different circumstances. They provide useful data for combustor design and optimization, and also for validating combustion models. However, only limited studies were conducted for measuring turbulent reacting flows in swirl combustors with staged air injection.

To meet the needs of developing swirl combustion technology leading to low NO_x emission, the turbulent swirling reacting flow in a combustor with staged air injection was experimentally studied recently. The instantaneous gas velocity is measured by utilizing a three dimension-laser particle dynamic analyzer (PDA). A flue gas analyzer was employed to measure the time-averaged gas temperature and species concentrations. The time-averaged gas axial and tangential velocities, temperature, and species concentrations and some of the statistical properties of the instantaneous gas velocity were reported in Ref.[13—15]. The obtained gas turbulence properties from the measurement are presented in this paper, including the PDF for instantaneous gas axial and tangential velocities, root mean square of axial and tangential fluctuating velocities, and second-order correlation moment for axial and tangential fluctuating velocities. These measured data may provide the basis for a better understanding of the turbulence and reaction mechanism of staged swirl combustion. They are also helpful to the formulation of theoretical model properly describing turbulence-reaction interactions.

2 EXPERMENTAL FACILITY

A test facility for swirl combustor was designed, fabricated, and set up. Fig.1 shows schematically the cylindrical swirl combustor with coaxial jets. The primary swirling air jet and the secondary non-swirling air jet are injected into the combustor through the inner and outer annular ducts, respectively, which forms a staged air injection. The gaseous fuel jet enters into the combustor through the coaxial center tube. A swirler with fixed vanes is placed in the inner annular duct to impart swirl to the primary air jet. The inside wall of the combustor is lined with refractory material to reduce heat loss to the surrounding. The inner diameter of the combustor is 160mm. The center fuel tube has an inner diameter of 8mm. The inner and outer diameters of the annular duct for the

---

Received 2005-08-23, accepted 2006-05-30.
* Supported jointly by the National Natural Science Foundation of China (No.59806006) and the Laboratory Open Fund of Tsinghua University.
** To whom correspondence should be addressed. E-mail: jianzhang@mail.tsinghua.edu.cn

primary air jet are 14 and 40mm, respectively. The annular duct for the secondary air jet has inner and outer diameters of 44 and 58mm, respectively. The length of the combustor is set at 1000mm. As shown in Fig.1, three windows, each with a length of 150mm and width of 95mm, are opened sequentially along the height of the combustor wall, where quartz glass is placed to allow the access of optical measurement.

A DANTEC PDA system was employed for the measurement of turbulent reacting gas flow in the swirl combustor. The PDA system includes an argon-ion laser, Bragg cell optical frequency shifter, transmitting optics, receiving optics, photomultipliers, three-dimensional traversing mechanism, data processor, and PC computer. The receiving optics collect signals in the backward scatter directions. The PDA makes use of the phase Doppler principle for simultaneous measurement of the instantaneous velocity as well as the size of seed particles in a flow field. The velocity measurement is based on the Doppler frequency shift of the signal scattered by the seed particles, while the size measurement is obtained from the phase shift among the scattered signals received by three photodetectors at separate spatial locations. The errors associated with the measurement of velocity and size of spherical seed particles are within 1% and 3%, respectively.

A small amount of seed particles has to be provided into the swirl combustor for the PDA experiment. The basic requirements for seed particles are high temperature endurance and free of agglomeration in reacting flows. Fine alumina (Al_2O_3) particles with nominal diameter of 3μm were chosen as seed particles in the present PDA measurement. The seed particles to be used in the experiment are placed in the bed of a fluidization feeder. During the measurement, a part of primary air is injected into the particle bed of the feeder. Some of the particles are elutriated to the freeboard of the fluidization feeder and may exit from the feeder with the entraining gas flow. The particles and air escaped from the feeder mix with another part of primary air and then they are injected together into the combustor. The gas flow rate through the particle feeder is cautiously controlled in the test to ensure sufficient PDA data collection rate and, in the mean time, to avoid particle contamination on the optical windows of the test section.

3 TEST CONDITIONS

PDA measurement of the instantaneous gas velocity was performed for three cases of turbulent reacting flow in the swirl combustor with staged air injection shown in Fig.1. The gaseous methane fuel with purity of 99.9% is axially injected into the combustor. Both air and methane are in the room temperature. The swirler is placed in the inner annular duct, which leads to swirling flow for the primary air jet. The secondary air jet through the outer annular duct is non-swirling. Table 1 lists the test conditions. It is seen that cases 1 and 2 are different in the total air flow rate, while the ratio of the secondary air flow rate to the total air flow rate is almost equal. Thus they have different axial velocities or Reynolds numbers for both primary and secondary air jets. Cases 1 and 3 differ in the ratio of the secondary air flow rate to the total air flow rate.

The instantaneous gas axial and tangential velocities were measured on four cross sections in the

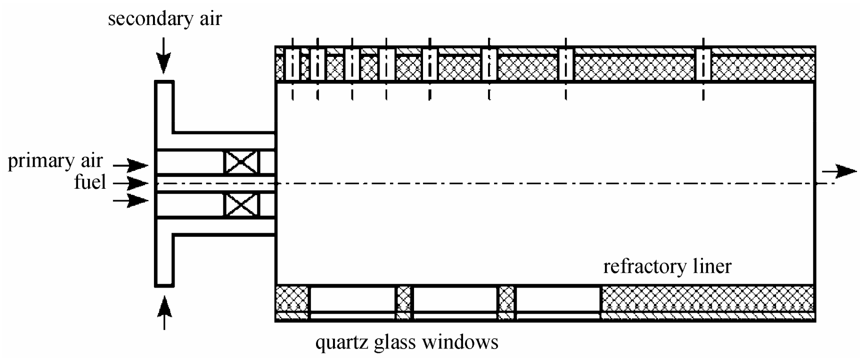

Figure 1 Swirl combustor with staged air injection

Table 1 Test conditions

Cases	Fuel flow rate, $m^3 \cdot h^{-1}$	Total air flow rate, $m^3 \cdot h^{-1}$	Ratio of secondary air flow rate to total air flow rate, %	Swirl number for primary air jet	Axial velocity of primary air jet, $m \cdot s^{-1}$	Axial velocity of secondary air jet, $m \cdot s^{-1}$	Reynolds number for primary air jet
Case 1	0.52	9.2	32.6	0.69	1.562	0.743	2870
Case 2	0.52	6.0	33.3	0.69	1.008	0.495	1850
Case 3	0.52	8.3	19.3	0.40	1.688	0.396	3100

swirl combustor. They are located at x/R=0.69, 1.06, 1.81, and 3.19, respectively. It is noted that the axial coordinate (x) starts from the inlet plane of the combustor and R represents the inner radius of the combustor. On each cross section, the gas velocity was measured at nine different radial locations from the central axis to the wall with the interval of 10mm. The total number of data to be sampled by the PDA is set at 3000 or the consecutive sampling time is set to be 360s for each measuring location in the present test. The measurement performed at each location should satisfy either of these criterions. As a result, the number of effective data taken by the PDA exceeds 1500 at most of the measuring locations. Thus, the statistical turbulence properties of the flow field could be obtained from the measured data of instantaneous gas velocity.

The agglomeration of seed particles could not be fully eliminated in the reacting flow with high gas temperature. The agglomerated particles with large size do not follow the gas flow closely. To reduce the errors for the gas flow measurements, the data taken from the seed particles with relatively large size are excluded in the PDA data processing. While only the data provided by the seed particles with diameters of less than 20μm are processed presently. These particles have a mean diameter of around 10μm and their velocities are much close to and can be taken as the gas velocities.

4 RESULTS AND DISCUSSION

From the measured time series data of instantaneous gas axial and tangential velocities by the PDA, the probability density functions for the instantaneous gas axial and tangential velocities at each measuring location are statistically obtained. Figs.2(a)-2(b) and 3(a)-3(b) depict the PDF for the gas axial velocity on the cross sections of x/R=0.69, 1.06, 1.81, and 3.19 respectively for Case 1. The radial coordinate (r) shown in these figures starts from the central axis of the combustor. It is seen from these figures that the PDF for the instantaneous gas axial velocity at each measuring location is approximately a Gaussian distribution. However, the PDFs exhibit different patterns and peak values at different locations. On the same cross section, the peak value of the PDF for the gas axial velocity decreases with decreasing radial distance. The instantaneous gas axial velocity becomes scattered as the radial distance decreases. Thus the turbulent fluctuation for the gas axial velocity is relatively strong in the central region. On the same radial locations near the combustor wall, the peak value of the PDF for the gas axial velocity exhibits a gradual decrease with the axial distance. The instantaneous gas axial velocity becomes increasingly scattered as the axial distance increases. Consequently, the turbulent fluctuation for the gas axial velocity increases gradually along the axial direction in the near wall region. The PDFs shown in Figs.2,3 suggest that the gas axial velocity has relatively large fluctuations in the central and downstream regions of the combustor.

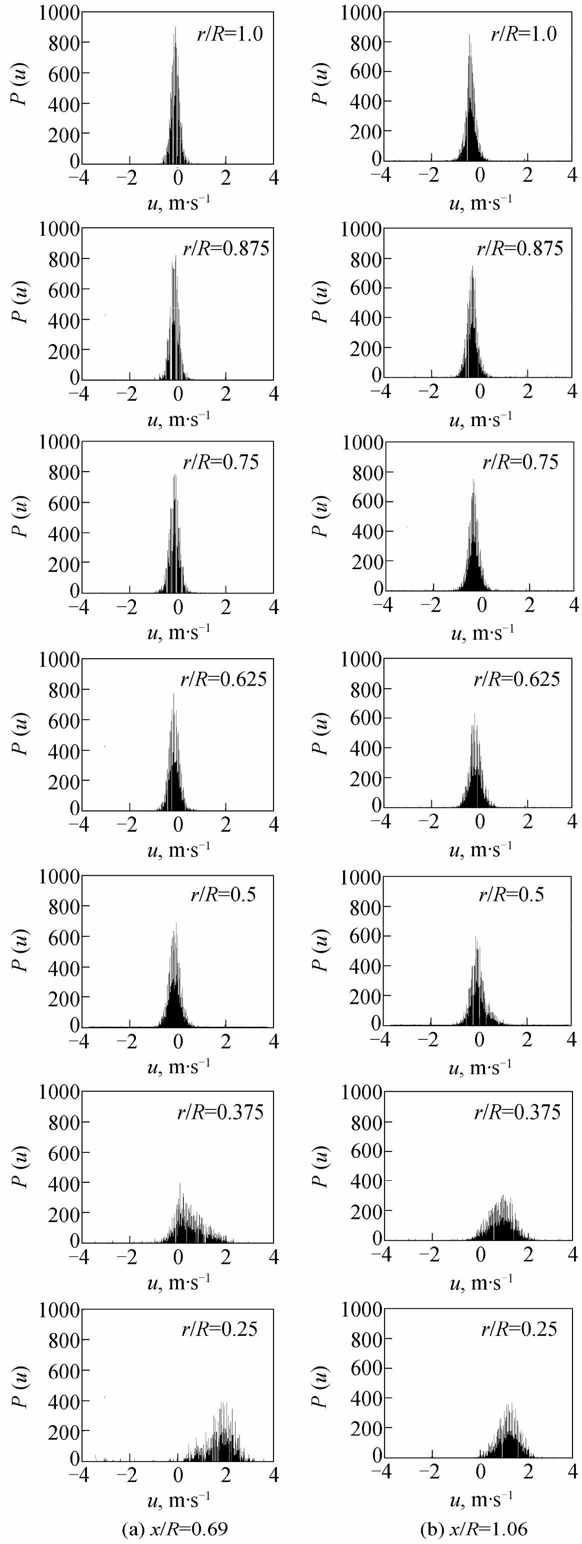

Figure 2 PDF for the instantaneous gas axial velocity at x/R=0.69 and 1.06 for Case 1

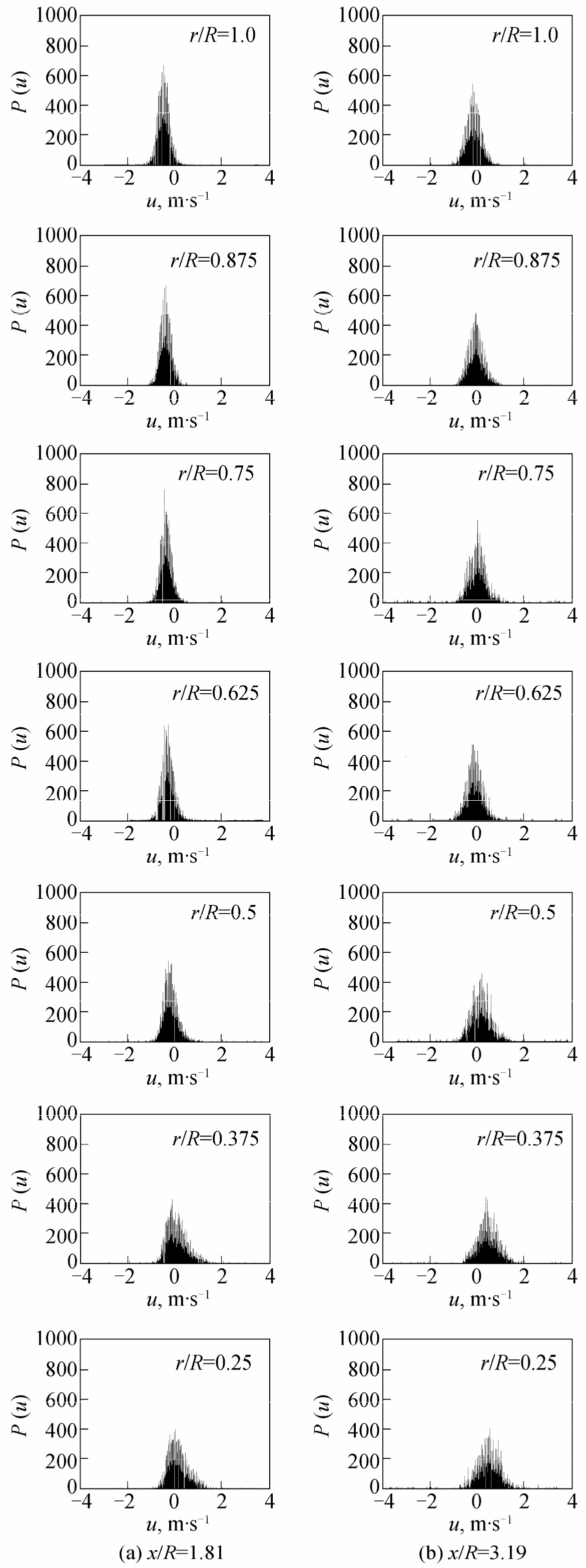

Figure 3 PDF for the instantaneous gas axial velocity at x/R=1.81 and 3.19 for Case 1

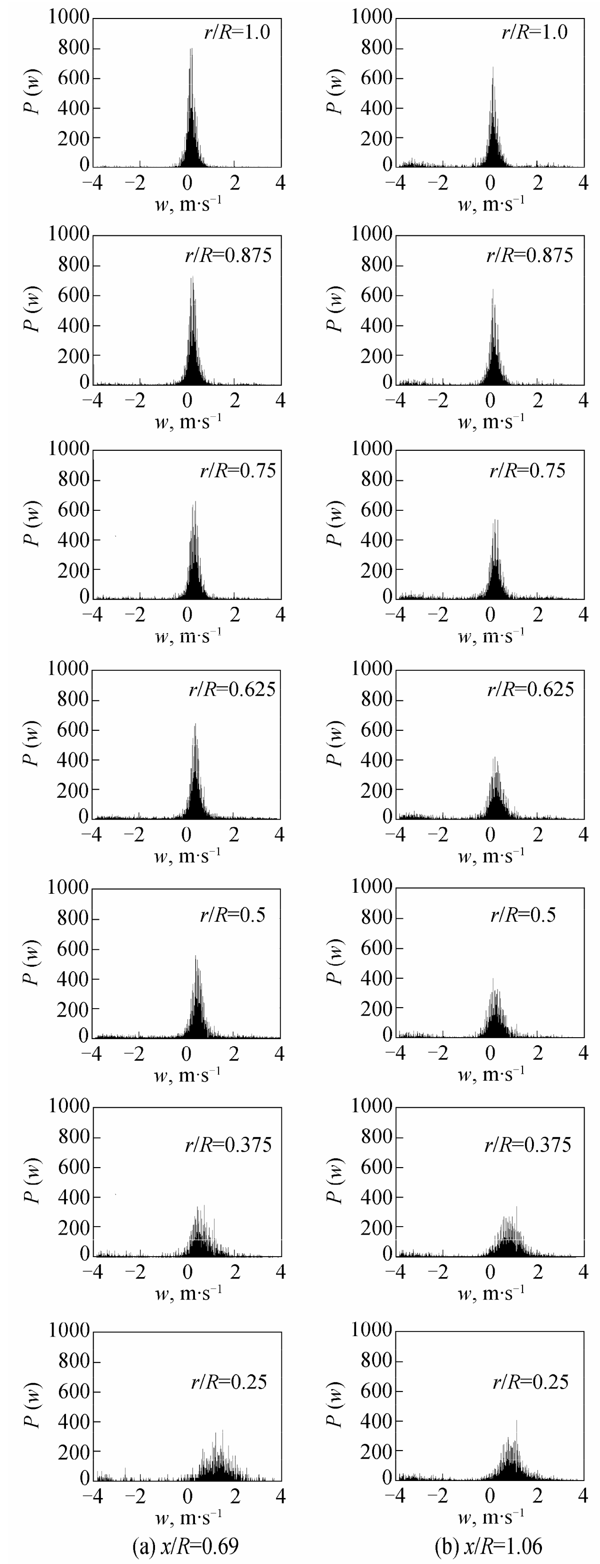

Figure 4 PDF for the instantaneous gas tangential velocity at x/R=0.69 and 1.06 for Case 1

Figures 4(a), 4(b) and 5(a), 5(b) present the PDF for the instantaneous gas tangential velocity on the cross sections of x/R=0.69, 1.06, 1.81, and 3.19, respectively for Case 1. In general, the PDF for the gas tangential velocity at each measuring location is close to a Gaussian distribution. However, the peak value of the PDF for the gas tangential velocity is lower than that for the gas axial velocity at the same location. The instantaneous gas tangential velocity is obviously more scattered than the instantaneous gas axial velocity. As

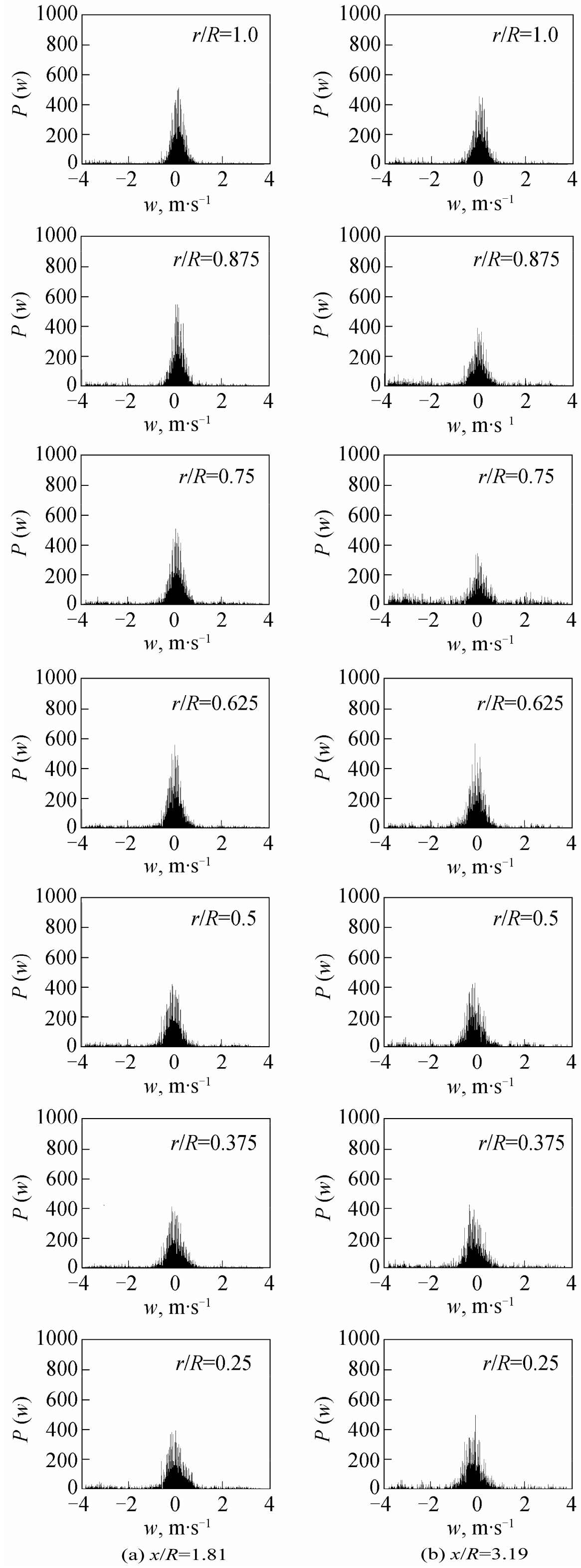

Figure 5 PDF for the instantaneous gas tangential velocity at *x*/*R*=1.81 and 3.19 for Case 1

a result, the turbulent fluctuation for the gas tangential velocity is larger than that for the gas axial velocity. In the upstream region of the combustor, the peak value of the PDF for the gas tangential velocity is seen to decrease with decreasing radial distance on the same cross section. The instantaneous gas tangential velocity tends to be increasingly scattered as the radial distance decreases, indicating that the turbulent fluctuation for the gas tangential velocity is relatively strong in the upstream central region. It is seen that the PDF for the gas tangential velocity deviates from the Gaussian distribution on the downstream cross section of *x*/*R*=3.19, where the instantaneous tangential velocity tends to be much more scattered and the turbulent fluctuation for the gas tangential velocity becomes large. Thus the fluctuation for the gas tangential velocity shows a more complex pattern than that for the gas axial velocity in the present case of swirling reacting flow.

The root mean square of fluctuating gas axial and tangential velocities and the second-order moment for the gas axial and tangential fluctuating velocities are further yielded from the measured instantaneous gas axial and tangential velocities. Fig.6(a) shows the distribution of the root mean square of fluctuating gas axial velocity for Case 1. It is seen that the fluctuating gas axial velocity is relatively high in the central region and low in the near wall region. The peak in its profiles is located in the central region, where the initial mixing and combustion occurs. Along the flow direction, the fluctuating axial velocity in the near wall region increases gradually, while the peak value in the profiles experiences no obvious change. It is seen that the profile of the fluctuating gas axial velocity tends gradually to be uniform in the downstream region. Thus the strength of the axial velocity fluctuation is generally maintained and even enhanced due to the staged combustion and flame expanding.

Figure 6(b) presents the distribution of the root mean square of fluctuating gas tangential velocity for Case 1. The fluctuating gas tangential velocity is relatively high near the central axis and low near the wall in the upstream region. It experiences large variations along the flow direction. Its magnitudes become large in the downstream cross section of *x*/*R*=3.19, where two peaks in the profile are found near the axis and the wall. The results imply that the circumferential flow may contain some large-scaled fluctuation as a result of flame expanding and staged combustion. Comparing Fig.6(b) with Fig.6(a), it is seen that the magnitude of the fluctuating gas tangential velocity is obviously larger than that of the fluctuating axial velocity. Thus the gas turbulence exhibits a non-isotropic feature in the swirling reacting flow.

Figure 6(c) shows the distribution of the second-order moment for the gas axial and tangential fluctuating velocities or the axial-tangential Reynolds shear stress ($\overline{u'w'}$) for Case 1. The absolute magnitudes of $\overline{u'w'}$ are relatively high in the initial central region and low in the near wall region, indicating that the shear stress and turbulent transport is relatively

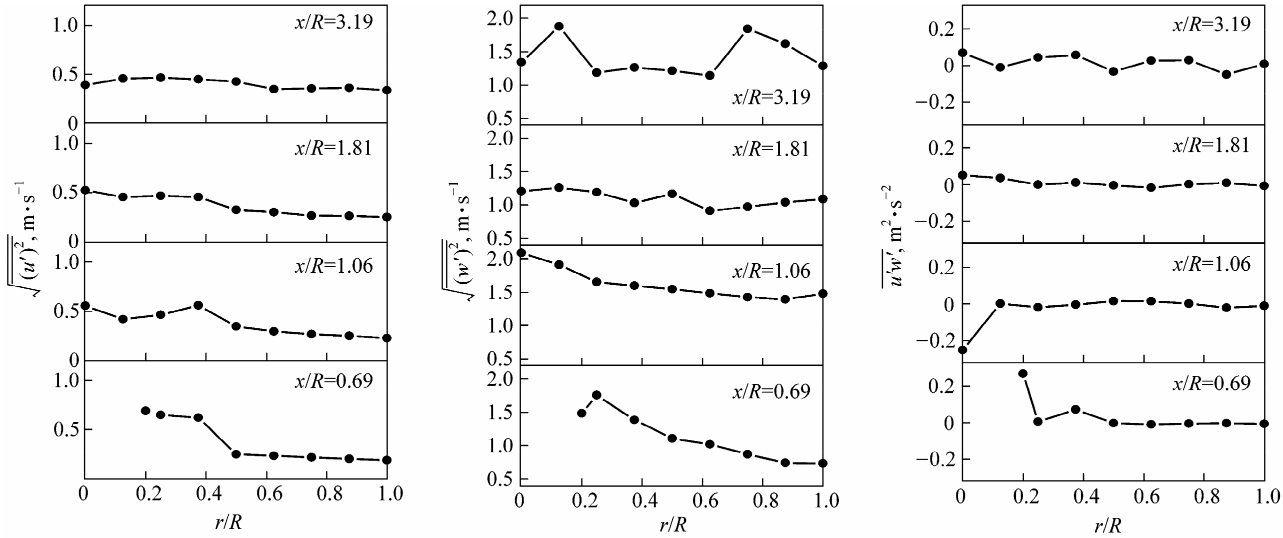

(a) Fluctuating axial velocity (b) Fluctuating tangential velocity (c) Axial-tangential Reynolds shear stress

Figure 6 Fluctuating gas axial and tangential velocities and second-order moment for the fluctuating gas axial and tangential velocities for Case 1

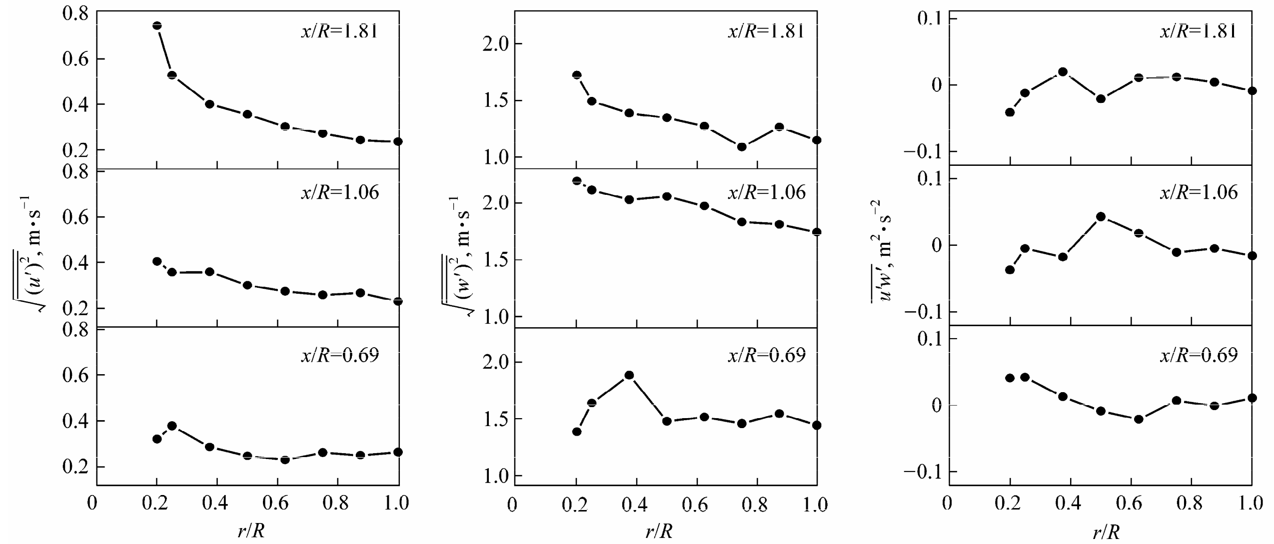

(a) Fluctuating axial velocity (b) Fluctuating tangential velocity (c) Axial-tangential Reynolds shear stress

Figure 7 Fluctuating gas axial and tangential velocities and second-order moment for the fluctuating gas axial and tangential velocities for Case 2

strong in the initial central region. It is seen that the magnitude of $\overline{u'w'}$ decays gradually along the flow direction and approaches zero on the cross section of x/R=1.81. However, the absolute magnitude of $\overline{u'w'}$ becomes relatively large again on the downstream cross section of x/R=3.19 due to the staged combustion.

Figures.7(a)—7(c) present the radial profiles of the root mean square of fluctuating gas axial and tangential velocities and the gas axial-tangential Reynolds shear stress for Case 2. This case has relatively lower Reynolds numbers for the primary and secondary air jets than Case 1. It is seen that the fluctuating gas axial and tangential velocities are high in the central region and relatively low in the near wall region. The peak in the profile of the fluctuating gas axial velocity increases along the flow direction as a result of staged combustion. The fluctuating gas tangential velocity experiences quite complex variation along the axial direction. Its magnitude is several times larger than that of the fluctuating gas axial velocity. The gas axial-tangential Reynolds shear stress is relatively strong in the central region and weak in the near wall region.

Figures.8(a)—8(c) show the radial profiles of the root mean square of fluctuating gas axial and tangential velocities and the axial-tangential Reynolds shear stress for Case 3. The ratio of the secondary air flow rate to the total air flow rate for this case is lower than

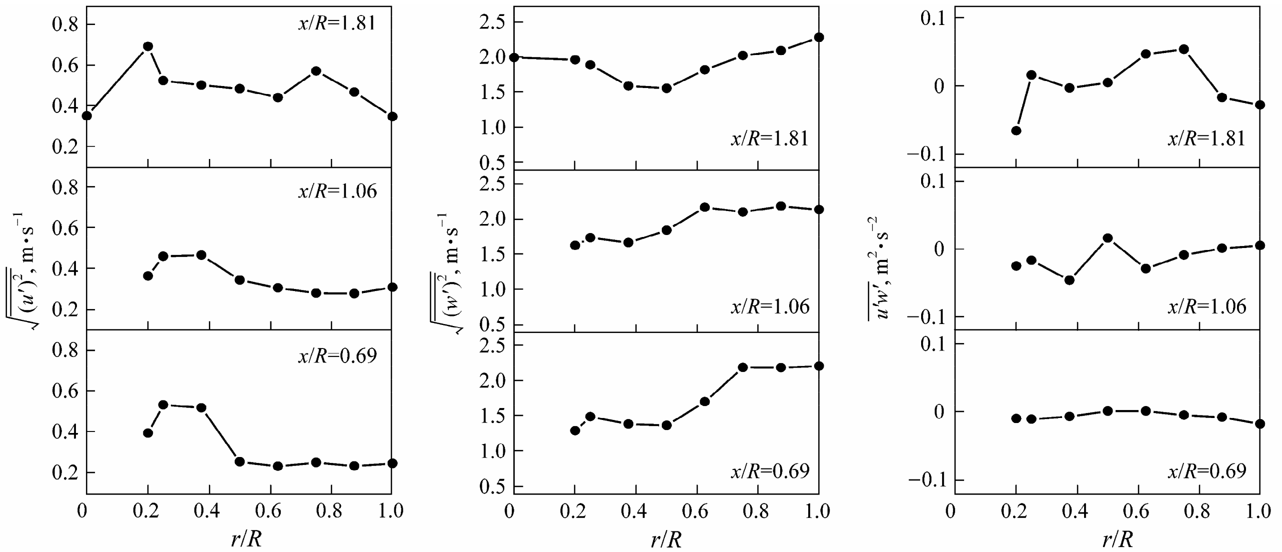

Figure 8 Fluctuating gas axial and tangential velocities and second-order moment for the fluctuating gas axial and tangential velocities for Case 3

that for Case 1. The staged air injection becomes relatively weak. The peak in the profile of the fluctuating gas tangential velocity is located near the wall. Its variation is not quite obvious along the axial direction. The profile of the fluctuating gas axial velocity has a peak near the central axis. As a result of staged combustion, the fluctuating gas axial velocity experiences large variation and tends to increase along the flow direction. The axial-tangential Reynolds shear stress is weak in the initial region and becomes relatively strong in the downstream region.

5 CONCLUSIONS

The turbulent reacting flow in a swirl combustor with staged air injection is experimentally studied. The measurement by the PDA provides the detailed turbulence properties of the combustion processes. They are summarized as below:

(1) The probability density function for the gas axial velocity is close to a Gaussian distribution. The PDF for the gas tangential velocity is also approximately a Gaussian distribution in the upstream region of the combustor. However, the PDF for the gas tangential velocity deviates from the Gaussian distribution in the downstream region.

(2) The fluctuating gas axial velocity and the absolute magnitude of the axial-tangential Reynolds shear stress are relatively high near the central axis and low near the wall. The fluctuating gas axial and tangential velocities remain strong in the downstream region due to the staged combustion. The absolute magnitude of the axial-tangential Reynolds shear stress becomes relatively large in the downstream region.

(3) The fluctuating gas tangential velocity is several times larger than the fluctuating gas axial velocity. The gas turbulence exhibits an obvious non-isotropic feature in the swirling reacting flow.

ACKNOWLEDGEMENTS

The help from Prof. Yan Dezhong and Prof. Li Yan of the Key Laboratory for Thermal Science and Power Engineering of Ministry of Education, Tsinghua University is acknowledged.

REFERENCES

1 Syred, N., Beer, J.M., "Combustion in swirling flows: a review", *Combust. Flame*, **23**, 143—201(1974).
2 Gupta, A.K., Lilley, D.G., Syred, N., Swirl Flow, Abacus Press, Tunbridge Wells, England (1984).
3 Smart, J.P., Weber, R., "Reduction of NO_x and optimization of burnout with an aerodynamically air-staged burner and an air-staged precombustor burner", *J. Inst. Energy*, **62**, 237—245(1989)
4 Zeng, H.C., Combustion and Pollution, Press of Huazhong University of Science and Technology, Wuhan, China (1992). (in Chinese)
5 LaRue, J.C., Samuelsen, G.S, Seiler, E. T., "Momentum and heat flux in a swirl-stabilized combustor", In: Proc. of 20th Symp. (Int.) on Combustion, The Combustion Institute, 277—285(1984).
6 Gouldin, F.C., Depsky, J.S., Lee, S.L., "Velocity field characteristics of a swirling flow combustor", *AIAA J.*, **23**, 95—102(1985).
7 Brum, R.D., Samuelsen, G.S., "Two-component laser anemometry measurements of non-reacting and reacting complex flows in a swirl-stabilized model combustor", *Exp. Fluids*, **5**, 95—102(1987).
8 Charles, R.E., Samuelson, G.S., "An experimental data base for the computational fluid dynamics of combustors", *ASME J. Eng. Gas Turbines Power*, **111**, 11—14(1989).
9 Hedman, P.O., Warren, D.L., "Turbulent velocity and temperature measurements from a gas-fueled technology

combustor with a practical fuel injector", *Combust. Flame*, **100**, 185—192(1995).
10 Anand, M.S., Takahashi, F., Vangsness, M.D., Durbin, M.D., Schmoll, W.J., "An experimental and computational study of swirling hydrogen jet diffusion flames", *ASME J. Eng. Gas Turbines Power*, **119**, 305—314(1997).
11 Vanoverberghe, K.P., Van Den Bulck, E.V., Tummers, M.J., "Confined annular swirling jet combustion", *Combust. Sci. Tech.*, **175**, 545—578(2003).
12 Anacleto, P. M., Fernandes, E. C., Heitor, M. V., Shtork, S. I., "Swirl flow structure and flame characteristics in a model lean premixed combustor", *Combust. Sci. Tech.*, **175**, 1369—1388(2003).
13 Pu, Y., Zhang, J., Zhou, L.X., "Experimental study of turbulent combustion in a swirl combustor using PDA", *J. Eng. Thermophys.*, **23**, 394—396(2002). (in Chinese)
14 Pu, Y., Zhang, J., Zhou, L. X., "Effects of staged air injection on the turbulent combustion in a swirl combustor", *J. Eng. Thermophys.*, **25**, 174—176(2004). (in Chinese)
15 Zhang, J., Pu, Y., Zhou, L.X., "Measurement of PDF for the instantaneous gas velocity in swirling turbulent combustion", *J. Eng. Thermophys.*, **25**, 707—710(2004). (in Chinese)